CNCs and CeO_2 as organic-inorganic additives to enhance HPC bio-polymer wood coatings against photochemical degradation.

Danial Harandi [a], *Zarah Walsh-Korb* [b], *Monireh Moradienayat* [a]*,

[a] Tabriz Islamic Art University, Department of Conservation and Archaeometry, Faculty of Cultural Materials Conservation, P.O. Box.15385-4587, Iran

Iran. d.harandi@tabriziau.ac.ir , monireh.moradie@gmail.com

[b] Department of Chemistry, University of Basel, 4058 Basel, Switzerland

zarah.korb@unibas.ch

ABSTRACT

Wooden objects of cultural heritage are susceptible to photochemical deterioration when exposed to UV radiation in outdoor environments, which results in the loss of their beauty and historical value. There is increasing interest in the field of wood conservation in studying biopolymers and bio-nanocomposite materials that have better characteristics and more compatibility with the wood components, thus, are more likely to give positive long-term conservation outcomes. This article focuses on the preparation of organic-inorganic bio-nanocomposite thin film coatings from hydroxypropyl cellulose (HPC), nanocrystalline cellulose (CNCs), and cerium nanoparticles (CeO2) applied using solution blow spraying (SBSp) to protect wood surfaces outdoors.

The uniform coating of nanocomposites and the thin film formation of this novel bio-nanocomposite on the wood surface were characterized by SEM imaging. The FTIR spectra of the films show that not only do CNCs improve the stability of HPC against UV radiation, but adding CeO2 nanoparticles further optimized the UV resistance of the bio-nanocomposites. ATR analysis of treated wood surfaces shows a decrease in the formation of hydroxyl groups due to photo-oxidation for both HPC/CNC treatments and the organic-inorganic bio-nanocomposite HPC/CNCs/CeO2 NPs. These results were also verified by colorimetric analysis. The UV-Vis spectra of the bio-nanocomposites showed that they absorb primarily in the UV-A and UV-B regions. Furthermore, the band gap was narrowed by adding CeO2 NPs to the HPC matrix, leading to enhanced UV resistance thin films.

KEYWORDS: *Wood, Bio-Nanocomposite Coatings, Nanocellulose, Nano Cerium, UV Resistance, Wettability.*

1. INTRODUCTION

Wood is the most versatile and widely available renewable resource, which has been utilized throughout history as a structural material, and for wooden artifacts1-4. Although wood is a durable material, unprotected wood is subject to surface degradation and photo-oxidation due to its biological nature 5-6. While wooden objects in controlled museum environments benefit from specific lighting and humidity settings, there exists a significant challenge in preserving larger heritage structures and outdoor wooden artifacts exposed to uncontrolled environments. Photodegradation is the fastest and most powerful environmental deterioration of wood7 and short-wavelength light is absorbed by a number of wood components, particularly lignin (between 295 and 400 nm), which becomes yellow and brown due to degradation of chromophoric structures and formation of secondary chromophoric ones 7. This is where our proposed material plays a crucial role, offering protection against

photodegradation and environmental factors. Different wood modification methods are used to improve wood surface properties such as thermal and chemical modification, which result in a change to the chemical nature of the wood8-9. Furthermore, many of these chemical treatments are not reversible and/or are too harsh on already fragile wood components to be considered for application on historical wooden artifacts. For instance, thermal treatment may affect the cell wall structure, in particular the crystalline part of the cellulose in soft and hardwoods 10, limiting its potential use in wood conservation.

Polymer-based coatings, primarily poly(ethylene glycol), epoxies or acrylics, are frequently applied as superficial wood treatments or through impregnation to delay the processes of wood degradation caused by UV light, moisture, and environmental factors 11-13. However, transparent coating techniques that maintain the natural properties of wood such as color, and texture have a limited life span when subjected to uncontrollable outdoor conditions 14. In particular, acrylic-based wood coatings, such as Paraloid-B72, reveal poor durability under outdoor light exposure 15. Preparations of polymeric-nanocomposites and nanoparticles dispersed in the polymer matrix are gradually emerging as viable alternatives to pure synthetic polymers and commercial polymeric coatings 15. Polymeric nanocomposites, with their heightened UV stability due to integrated nanoparticles, offer a resilient shield against wood degradation in uncontrolled outdoor settings. Their potential lies in significantly prolonging the stability of wood treatments, ensuring enduring protection against the detrimental impact of unpredictable light exposure.

One innovative treatment approach involves organic-inorganic nanocomposites, a class of materials showing great potential for conservation applications due to their enhanced durability, high performance in mechanical and thermal properties, and versatility 16-17. In the context of cultural heritage preservation, there is growing interest in incorporating both inorganic and organic nanoparticles into polymer matrices. In cultural heritage preservation, nanoparticles in polymer matrices serve functions beyond acid neutralization and anti-bacterial properties, including UV protection, hydrophobicity, mechanical reinforcement, self-cleaning, thermal stability, and color retention. Various nanoparticles, including calcium (Ca), magnesium (Mg), silver oxide (Ag2O), copper (I) oxide (CuO), zinc oxide (ZnO), and titanium dioxide (TiO2), have been explored in the literature 18-19. Recent studies have highlighted the effectiveness of nano-ZnO in enhancing weathering resistance and water absorption of wood 20. Furthermore, nano-ZnO has been used as an additive in Paraloid B72, leading to improved hydrophobicity of the consolidant 21. Combining nano-ZnO with Ag NPs has also demonstrated protection against UV irradiation, microbial infestations, and increased mechanical stability 22.

Cellulosic materials have risen in prominence in recent years due to their biodegradability, low environmental impact, biocompatibility, customizable optical properties, and stable performance, aligning with the growing demand for eco-friendly products 23. Cellulose derivatives, primarily obtained from biomass through cost-effective chemical modification, hold promise in various applications. Cellulose derivatives like hydroxypropyl cellulose (HPC) are favored for wood conservation due to their biocompatibility, and they have found application as effective consolidants, adhesives, and coating materials for a range of organic materials such as wood 24, paper 25, and leather 26. HPC is notable among cellulose derivatives because it can dissolve in both water and organic solvents, making it versatile for various applications. Its hydrophilicity, ease of processing, and unique

phase behavior contribute to its wide range of uses 27. However, HPCs weak mechanical properties pose challenges for conservators dealing with highly damaged artifacts 28-29. Incorporating CNCs into the HPC significantly enhances the coating's strength, rigidity, and dimensional stability 30. The wood structure is reinforced and its overall durability and resistance to environmental factors, such as UV radiation and moisture, are augmented by the penetration of nano-sized fibers of CNCs. 31-32.

However, considering outdoor applications, CNCs do not provide optimal resistance to UV-induced degradation processes. To enhance UV-blocking capabilities and overall wood conservation for outdoor settings, the integration of cerium oxide nanoparticles (CeO2 NPs) is a promising strategy. CeO2 NPs possess the ability to absorb and scatter UV radiation, providing an additional layer of defense against the detrimental effects of ultraviolet light on wood surfaces 33-36. However, potential toxicity issues associated with CeO2 NPs must be considered. Existing research indicates that the toxicity of these nanoparticles can vary significantly based on concentration, exposure time, and the specific cell lines studied. As the focus lies on optimizing the concentration of CeO2 NPs for effective UV protection, a comprehensive toxicity assessment will be integral to further study.

This study was initiated to assess the potential of CNCs and CeO2 NPs, and combinations of the two, as additives to enhance the properties of HPC, creating an organic-inorganic bio-nanocomposite treatment for the protection of wood surfaces in uncontrolled, primarily outdoor, environments. The treatments were applied on wood surfaces using a new technique known as solution blow spraying (SBSp). Proposing the use of SBSp to gently apply a polymer-based nanocomposite onto any surface. SBSp, known for its versatility, offers a convenient method to coat and treat surfaces. By spraying the polymer solution or suspension onto the desired surface, you can control the amount applied, regulating the thickness of the deposited material. Additionally, SBSp, especially in solution spraying techniques, has proven effective in producing polymer-based nanocomposites with an even dispersion of nanoparticles37.

The subsequent sections detail the experimental setup, materials, and SBSp methodology, followed by an analysis of results showcasing the synergistic effects of CNCs and CeO2 NPs. The study's outcomes contribute insights into developing advanced bio-nanocomposite treatments for wood protection, emphasizing SBSp's efficacy and the promising potential of CNCs and CeO2 NPs.

2. EXPERIMENTAL

2.1. Materials

Fir wood (Abies alba), with dimensions of 100 × 35 × 20 mm^3 (in the radial, tangential, and longitudinal directions, respectively), served as the substrate. The wood surfaces were sanded with H 240 grit sandpaper. Subsequently, they were placed in a controlled environment at a temperature of 20 ± 2 ◦C and a relative humidity (RH) of 67 ± 5 % until they achieved a stable weight, indicating an equilibrium water content of approximately 12 % by weight.

Hydroxypropyl cellulose, Klucel G, produced by C.T.S Spain was used as the polymer matrix. Cerium Oxide nanopowder (CeO2, 99.97%, 10-30 nm, CAS No: 1306-38-3) supplied by US Research Nanomaterials, Inc, and nanocrystalline cellulose (CNCs) in the form of 2.5% aqueous gel, (20–40 nm, purity ≥99.5 %), chemically synthesized by Nanonovin (Iran) were employed as the filler.

2.2. Samples Preparation and coating method

HPC, 2 wt.% was prepared in distilled water. Aqueous suspensions of 2 and 3 wt.% CeO2 NPs with a constant amount of 5 wt.% CNCs were subjected to ultrasound for 1 h. The NP/CNC suspension was added into the 2 wt.% HPC suspension in distilled water and stirred at room temperature for 30 min to fabricate the bio-nanocomposites. A volume of 2 mL of the bio-nanocomposite suspensions were applied on each wood specimen by a commercial airbrush and compressed air as presented in Figure 1,a) The Solution Blow Spraying (SBSp) process was conducted under the following conditions: nozzle diameter = 0.5 mm; fluid cup capacity = 5 cm^3; pressure = 2 bars, with a working distance of approximately 6 cm. Additionally, thin films were cast to investigate the optical properties, which were analyzed using UV-Vis spectrometry. Figure 1, b) displays cast pure HPC, and S2 shows HPC+CNCs films, which are nearly transparent. Addition of cellulose nanoparticles (CNCs) to the HPC matrix does not appear to reduce transparency to any great degree. However, when CeO2 nanoparticles are added to the polymer, there is a noticeable reduction in film transparency (S3, S4).

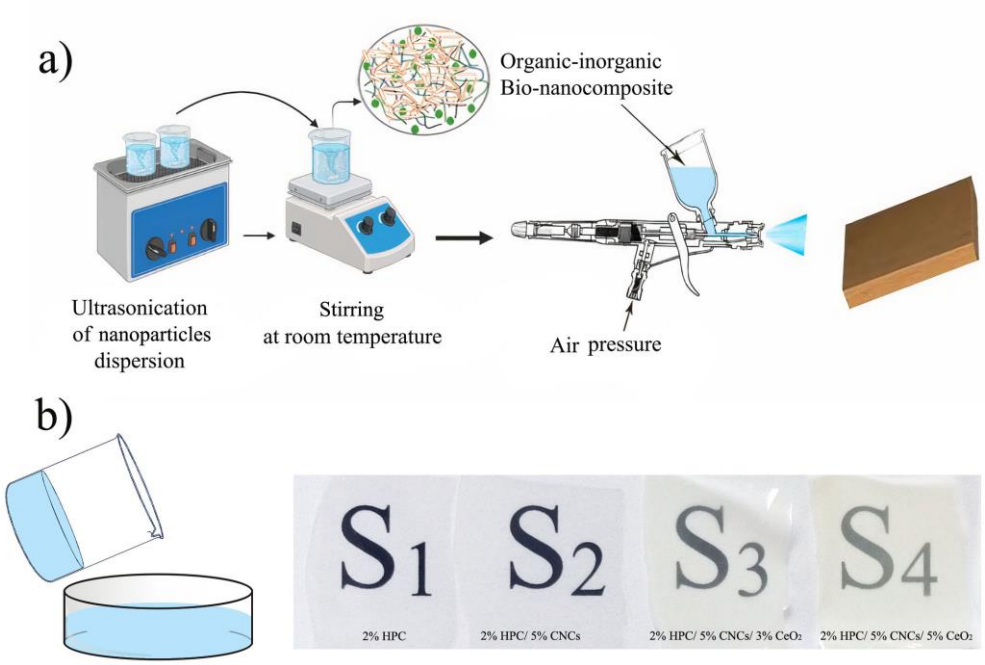

Figure1. Scheme view of HPC /CNCs/CeO_2 bio-nanocomposites applied by SBSp method on wood and thin films obtained by casting method.

2.3. Microscopic Investigation

A LEO 440-I scanning electron microscope (SEM), Carl Zeiss (Jena, DE), was utilized to assess the wood surface coating achieved through the SBSp method. This analysis also focused on examining the morphology and distribution of the nanocomposite coatings on the wood substrate.

2.4. UV resistance tests

To evaluate the UV protection effectiveness of the composite coating applied to wood specimens measuring 100 × 35 × 20 mm^3, an irradiation source featuring UV-A lamps (wavelength of 370 nm) (Philips, Narva, LT 18w/073) was employed. All samples were positioned at a distance of 15 cm from the lamp and exposed at room temperature for a total duration of 240 h. Bio-nanocomposite films were exposed to UV light for 480 h under the same conditions as the wood samples.

2.5. Color measurements

The color parameters L* (representing lightness), a* (indicating redness), and b* (reflecting yellowness), along with the color change indices (ΔL*, Δa*, Δb*, and ΔE*), were quantified in each sample both prior to and following the aging process, utilizing the CIE LAB color system. The overall color change, denoted as ΔE*, was assessed using the following Eq [38]:

$$\Delta E = \sqrt{(\Delta L*)^2 + (\Delta a*)^2 + (\Delta b*)^2} \quad (1).$$

2.6. Wetting Capability

The evaluation of the wettability of the wood surface coated with the bio-nanocomposites under investigation involved measuring the static contact angle. This assessment was conducted using a water contact angle device (JIKAN-CAG-10, Iran). The static contact angle analysis was performed 1 s after releasing a 10 µl droplet of deionized water onto the wood surface.

2.7. Optical properties

The ultraviolet-visible (UV–Vis) spectra of the films were captured using an Avantes UV-VIS spectrometer (AveLight-DH-S-Bal, Netherlands), spanning the wavelength range of 200 – 800 nm.

To calculate the direct and indirect optical band gaps based on the UV−Vis Spectra, the Tauc technique was employed. The optical band gap is determined using the absorption coefficient (α) and the incident photon energy (hν) and can be expressed by following Eq. [39]:

$$(\alpha h\nu)^{1/n} = B(h\nu - E_g) \quad (2).$$

Where α, is the absorption coefficient; h is Planck's constant (6.626·10-34 J·s); ν the photon's frequency (in seconds); Eg the band gap energy; B is a constant number. The factor n depends on the nature of the electron transition and is equal to ½, for the direct transitions or 2 for the indirect transition band gaps [39].

To calculate the energy band gap (Eg) of the samples, the absorption coefficient (α) is calculated by Eq [40]:

$$\alpha = 2.303\left(\frac{A}{L}\right) \quad (3).$$

Where A, is absorbance and L, thickness of thin films.

The values of energy (hν) and, so the values of the energy band gaps were calculated using the following expression [41]:

$$E\ (eV) = \frac{1240\ (eV{\cdot}nm)}{\lambda\ (nm)} \quad (4).$$

To obtain the energy band gap, the straight-line portion of the curve of (αhν)2 vs hν for the direct band gap and (αhν)1/2 vs hν for the indirect band gap was extrapolated. [39].

2.8. Chemical characterization by FTIR

Fourier transform infrared (FTIR) spectroscopy of the films was conducted using a JASCO 680-plus spectrometer, with a spectral resolution of 4 cm^{-1} and an average of 32 scans. For the chemical characterization of the treated wood surface following UV aging, attenuated total reflectance

Fourier transform Infrared (ATR-FTIR) analysis was employed. This was performed using a JASCO 4700 spectrometer (USA) with an averaging of 32 scans and a resolution of 4 cm^{-1}.

3. RESULT AND DISCUSIONS

Figure 2, a) presents a comparison between the wood surfaces before and after treatment with the bio-nanocomposites under investigation, control treatments and an uncoated sample. It is noteworthy that, from an initial perspective, the wood surface appears to have been successfully coated with a transparent HPC/CNCs/CeO2 bio-nanocomposite film, and no alterations in the appearance of the wood specimens were detected. In Figure 2, a) the lower portion of the image showcases wood samples subjected to UV aging, demonstrating treatment with both pure HPC and its respective nanocomposites. The CIE L*a*b*color space coordinates were measured to monitor the color changes of the wood surfaces after 240 h of UV irradiation. In order to obtain more accurate results, the colorimetric values of each sample were individually compared with the parameters of the same sample before exposure to UV irradiation, as shown in Table 1. Figure 2, a) illustrates the colorimetric changes in wood samples before and after exposure to UV light. The untreated wood sample and the wood sample treated with pure HPC undergo significant color changes, becoming darker and more yellow compared to the others. The Δa* parameter of the HPC-coated sample showed a slight increase compared to uncoated wood. This change can be attributed to the simultaneous color shift of both polymer and wood to red. The yellowing of the exposed, uncoated wood surface occurs due to the formation of secondary carbonyl groups including quinoids, aromatic ketones, and aldehydes. This occurs as a result of lignin photodegradation, but it is limited to a depth of only 0.15 mm 42-44. Notably, the total color difference, denoted as ΔE*, decreased with the addition of 5% CNCs, approaching that of HPC alone. A comparison of the ΔE* values between the 2% HPC/5% CNCs/3% CeO2 and 2% HPC/5% CNCs/5% CeO2 samples indicates that, on the whole, the addition of CeO2 has effectively optimized color changes induced by UV radiation. Moreover, the increase in cerium content up to 5% within the HPC polymer played a role in reducing the photochemical degradation of wood surfaces treated with this innovative nanocomposite.

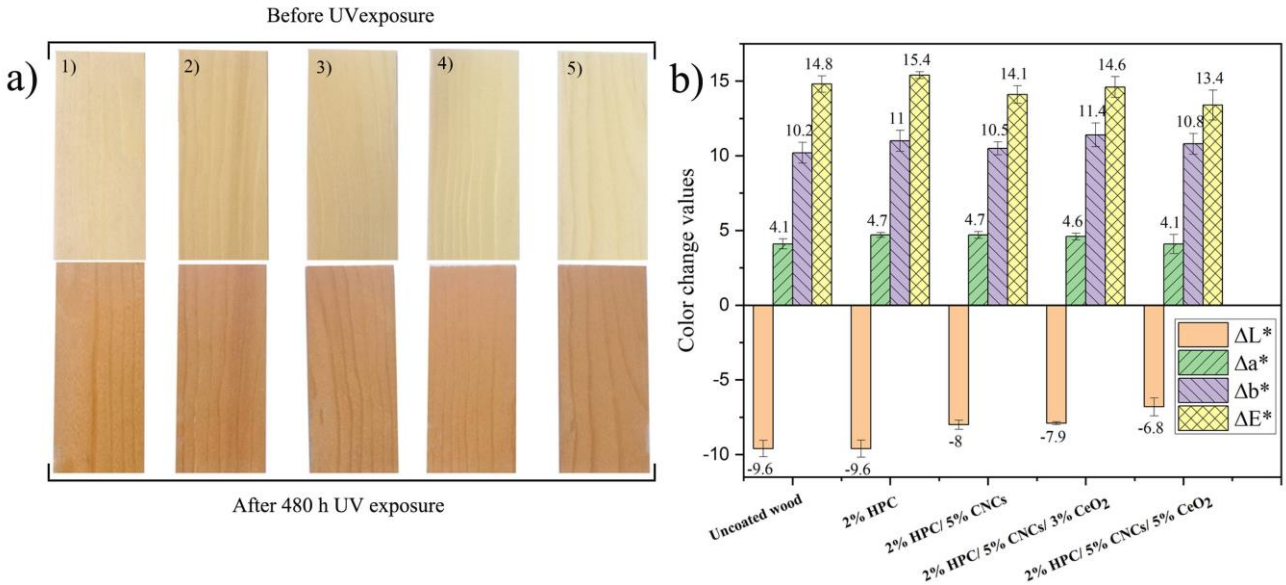

Figure 2: a) visual representation of the wood surfaces initial appearance before and after exposure to UV aging and b) Changes in Lightness (ΔL*), Redness (Δa*), Yellowness (Δb*), Total Color (ΔE).

Table 1. Colorimetric values (L*, a*, and b*), CIE of samples before and after irradiaion.

	*L**	*a**	*b**	*L**	*a**	*b**
		Before			**after**	
Untreated	84.2	5.3	17	74.5	9.4	27.3
2% HPC	80.6	6.9	20.5	71	11.6	31.6
2% HPC / 5% CNCs	82.1	6.1	20.9	74.1	10.9	31.5
2% HPC / 5% CNCs / 3% CeO_2	81.1	6.8	20.5	73.	11.5	31.9
2% HPC / 5% CNCs / 3% CeO_2	81.5	6.3	19.5	74.6	10.5	30.2

Figure 3 shows the surface morphology and deferent section view of wood surfaces treated with two bio-nanocomposite films. The wood coated with 2% HPC/5% CNCs is displayed at both low and high magnification (Figures 3a and 3b). This analysis unveiled a homogeneous nanocomposite layer on the wood surface, with a uniform dispersion of nanoparticles. When the wood is treated with the HPC/5% CNCs/5% CeO2 bio-nanocomposite, as illustrated in Figure 3c, it is evident that the nanoparticles are well embedded in the polymer matrix, providing comprehensive coverage of the wood surface. Since the bright spots corresponding to the CeO2 are uniformly distributed across the entire coated wood surface, it is reasonable to infer that the particles within the film used for wood coating are well-dispersed and homogeneous. Additionally, cross and radial section images of HPC/5% CNCs/5% CeO2 (Figures 3d-e) reveal the existence of a thin layer, measuring approximately 23 µm on the wood surface. This layer displayed notable homogeneity. Furthermore, in a high-magnification image (Figure 3f), it is apparent that the nanocomposite adhered securely to the wood surface.

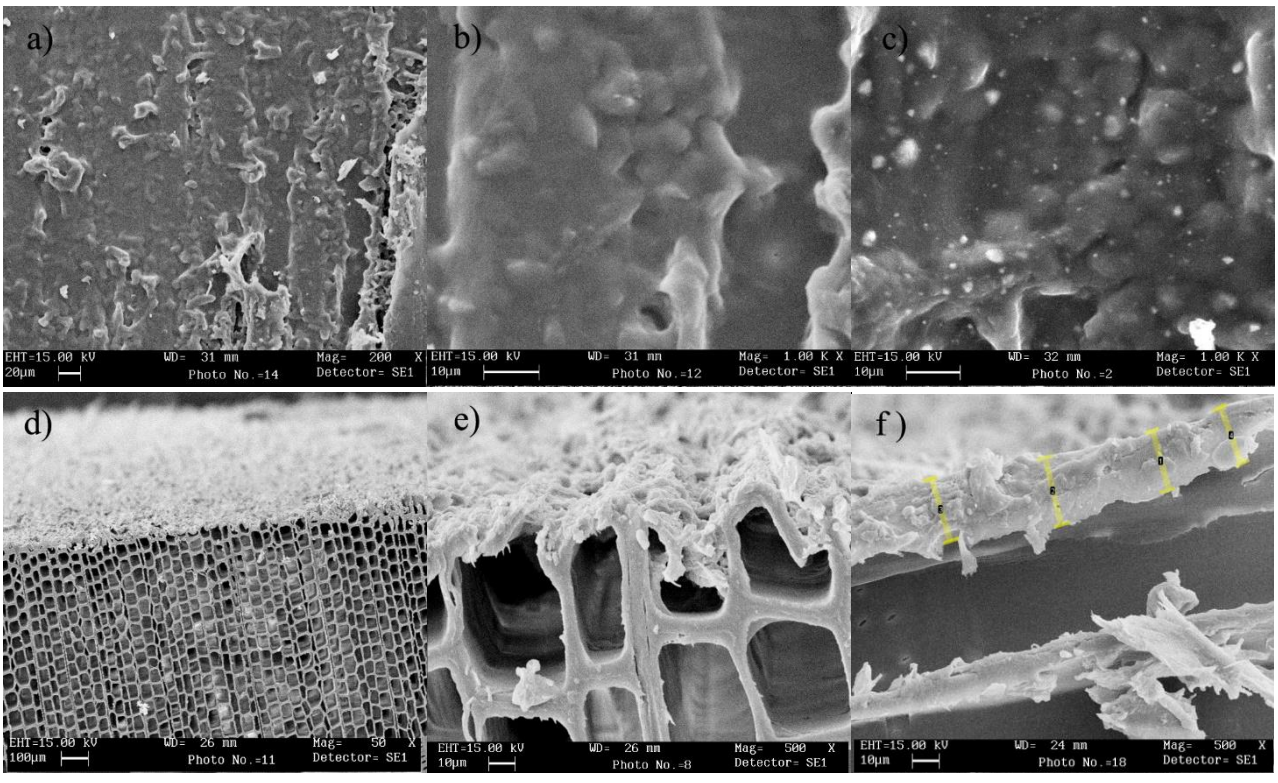

Figure 3: Scanning electron microscope images of (a-b) the surface of wood samples treated with 2% HPC/5% CNCs NPs, (c-f) surface, cross and radial section of coated wood with HPC/5% CNCs/5% CeO_2.

To examine the chemical changes in HPC and its bio-nanocomposites after extended UV exposure, FTIR spectra were recorded following 480 h of UV irradiation wavelength of 370 nm. Figure 4, a) depicts the comparative spectra obtained during accelerated UV aging. Notably, the bands within the 1079-1175 cm^{-1} range, associated with -C-O asymmetric stretching, and the band at 1449 cm^{-1}, signifying C=C stretching were observed to be dramatically increased in intensity. Furthermore, within the 1279 to 1344 cm^{-1} range, notable indications of heightened presence of -CH_2- methylene bridges were observed, particularly in pure HPC samples [41, 45]. Despite the reduction in the degree of photochemical degradation achieved through the preparation of polymer nanocomposites with cellulose and cerium, it's noteworthy that there was still a significant increase in the intensity of the sharp band at 1642 cm^{-1}, corresponding to the stretching vibration of C=O of the conjugated ketonic group. The increase was particularly prominent in pure HPC after the aging process [45] and less pronounced in the bio-nanocomposite films. Furthermore, a redshift in absorption at 1642 cm^{-1} was observed. The enhancement in intensity at this particular band was comparatively lower in the HPC/5% CNCs and HPC/5% CNCs/5% CeO_2 samples, in contrast to the pure polymer, indicating the prevention of the formation of carbonyl groups at 1734 cm^{-1} and 1642 cm^{-1}. It is interesting to note that the addition of 5 wt.% CNCs demonstrated UV resistance nearly equivalent to that of 5% CNCs/5% CeO_2. However, it's important to emphasize that the most effective protection against photochemical degradation is achieved with the lowest amount of cerium, underscoring the need to refrain from excessive CeO_2 content in HPC. The catalytic activity of cerium nanoparticles plays a pivotal role in mitigating photochemical degradation by participating in reactions that neutralize UV-induced degradation pathways. Optimal dispersion and interaction at lower cerium concentrations enhance desired properties, but higher concentrations of nanomaterial can produce a large amount of radicals, consequently contributing to the degradation of the HPC matrix[46].

Figure 4b compares the FTIR-ATR spectra of uncoated wood with HPC- and bio-nanocomposite-coated wood before and after 480 h of UV exposure. The band at 1506 cm^{-1}, corresponding to lignin, in the untreated wood sample was significantly reduced compared to the wood control sample after exposure to UV irradiation. [42-43] Across the bio-nanocomposite treated samples, the absorption of this band decreases after treatment. Hence, if this band in treated samples is compared after aging, it can be seen that less lignin degradation occurred in the HPC/CNCs/3% CeO_2 sample.

In uncoated wood, the band intensity at 1734 cm^{-1} corresponding to non-conjugated aliphatic carbonyls was also significantly increased after exposure to UV irradiation, indicating the formation of strong carbonyl compounds. Interestingly, it appears that adding 5 wt.% CNCs to the HPC is enough to prevent the formation of carbonyl groups. The bands at 1595 cm^{-1}, corresponding to C=C unsaturated linkages, and 1653 cm^{-1}, due to C=O stretching of conjugated or aromatic ketones, in the 5% CNCs and 5% CNCs/5% CeO_2 exhibit a slight increase in comparison to the uncoated wood and wood treated with HPC alone. It can be concluded that the incorporation of CNC nanofillers in HPC can protect of the wood against photochemical degradation, and cerium nanoparticles further optimized the properties of the bio-nanocomposites.

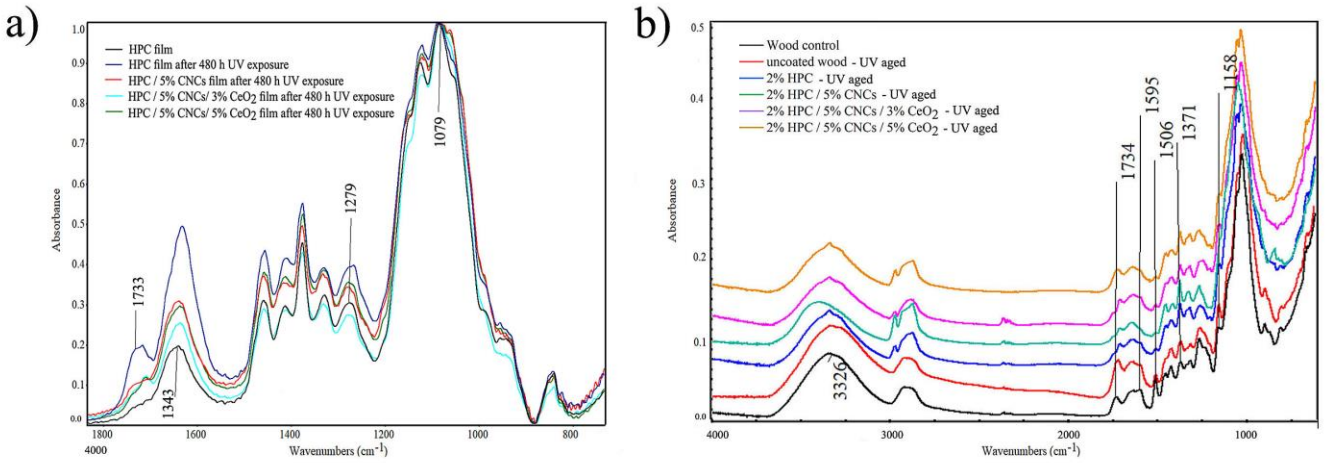

Figure 4: a) FTIR spectra Analysis of HPC and its bio-nanocomposites films after subjecting to UV irradiation, b) Comparison of FTIR-ATR spectra between untreated and treated wood with HPC and bio-nanocomposites after UV exposure.

The optical properties of the bio-nanocomposite films, as depicted in Figure 5a, were analyzed using UV-Vis spectroscopy. The optical absorption was increased by adding CNCs and CeO_2 nanoparticles as filler into the HPC matrix. In Figure 5a, it is evident that the HPC exhibits poor absorption at wavelengths between 200 and 800 nm. When CNCs were added to polymer, the intensity slightly increased and a small absorption peak was observed in the visible region between 400 and 500 nm. The addition of 3 wt.% CeO_2 filler into HPC/CNC bio-nanocomposite films results in a significant increase in absorption of UV-A (320-400) and UV-B (280-320) radiation, which increases further when the CeO_2 content is increased to 5 wt.% (2% HPC/5% CNCs/5% CeO_2). This indicates its potential as an effective UV absorber in bio-nanocomposite films. These films act as protective layers, shielding cultural artifacts from the detrimental effects of UV radiation, which can lead to fading, discoloration, and structural degradation over time.

The optical band gap energy obtained from the UV-VIS spectroscopy of films was determined using the Tauc method (Figure 5b). The bad gap energy is estimated to be 5.42 eV for pure HPC. This value is in accordance with the band gap energy that was reported in previous study of HPC [47]. It was decreased to 5.19 eV by adding CNCs into the matrix and wide band gap of HEC tends to be slightly narrowed. The band gap value is further reduced to 4.18 eV by the addition of 3 wt.% CeO_2. The CeO_2 nanofiller causes narrowing of the band gap energy in the HPC/CNC bio-nanocomposites [48] and it was further optimized to 3.46 eV by increasing the CeO_2 content in polymer matrix to 5 wt.%. It is noted that the absorbance and absorption coefficient in the UV–Vis range increase with a rise in the concentration of CeO_2 nanoparticles in the film. The decrease in the optical bandgap can be attributed to the inclusion of the local energy levels in the bandgap structure by CeO_2 structure.

Therefore, it can be explained that by increasing the nanoparticle concentration a narrower band gap is obtained, which leads to an enhancement of the photocatalytic activity[40, 49]. This improvement in photocatalytic properties could have significant implications for the preservation of wood artifacts exposed to uncontrolled environments.

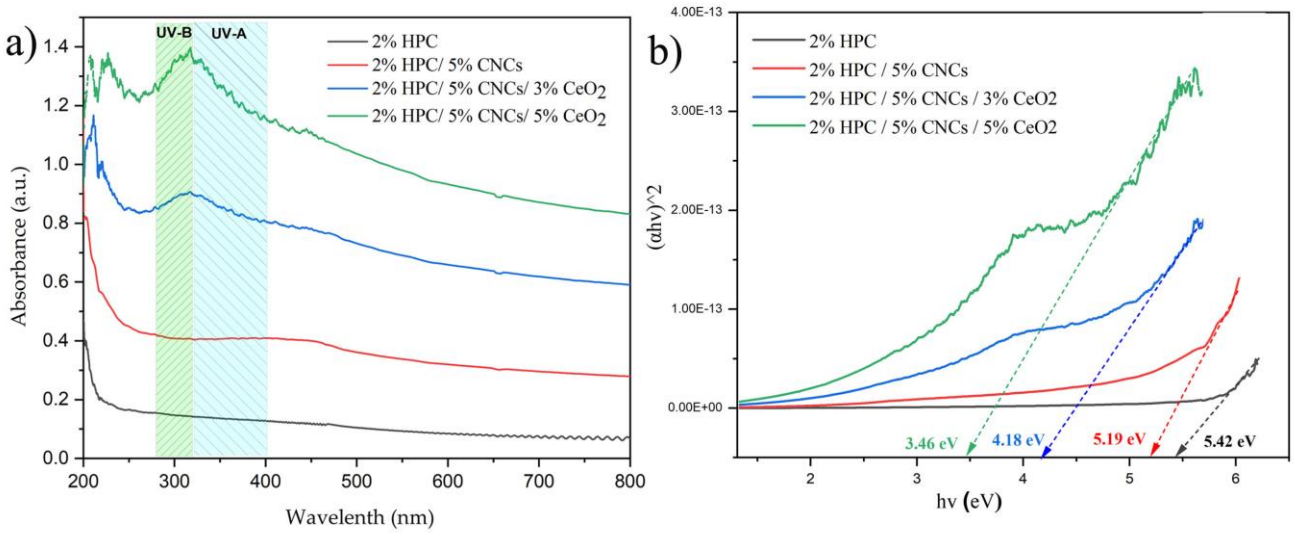

Figure 5: a) UV-visible absorption spectra and b) band gap energy obtained from UV- visible spectroscopy of HPC and its bio-nanocomposite films.

Figure 6 illustrates the static water contact angle measurements for untreated wood and samples treated with bio-nanocomposites. The water contact angle of untreated wood (a) significantly differs from that of the treated samples, which can be attributed to the greater availability of free hydrophilic hydroxyl groups on the wood surface [50-51]. A contact angle of approximately 69º was measured for samples treated with HPC, while, for samples treated with HPC/CNCs, the angle was approximately 64º. The addition of CNCs to HPC (c) resulted in a slight reduction in the water contact angle (WCA), indicating a modest decrease in surface hydrophobicity. The introduction of CeO_2 into the HPC/CNC nanocomposite had the effect returning the contact angle to that observed for pure HPC (d), reducing wettability. Interestingly, as more CeO_2 was incorporated into the nanocomposite (e), the WCA increased, leading to a reduced wettability, signifying enhanced hydrophobicity of the wood surface when coated with this novel organic-inorganic nanocomposite. The heightened hydrophobicity is beneficial, as it suggests improved water repellency, a desirable trait that may contribute to mitigating bacterial degradation and enhancing the overall durability of the treated material.

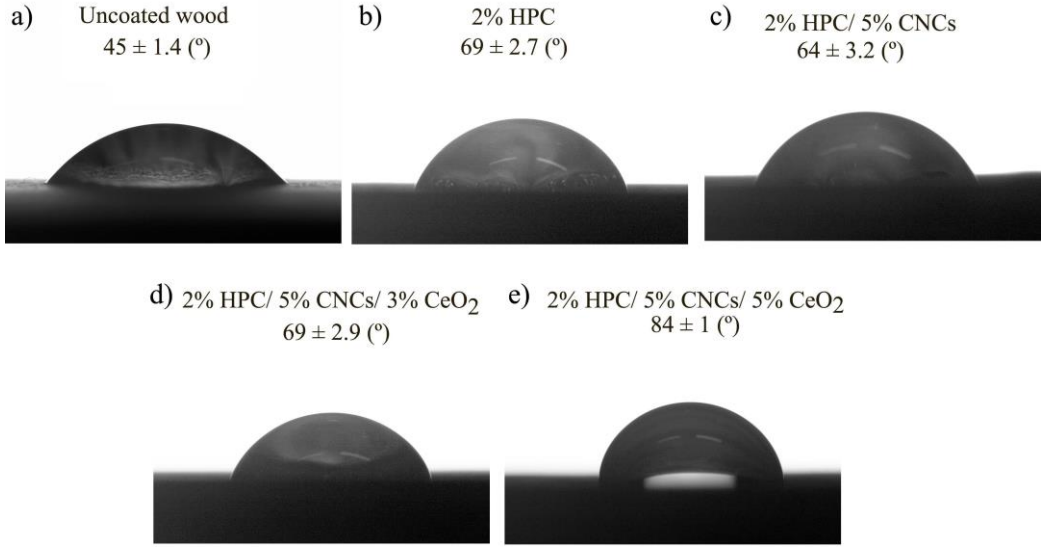

Figure 6: Water contact angle assessment of wood surfaces treated with HPC/CNCs/CeO_2 nanocomposite compared to un and neat HPC.

4. CONCLUSION

In this study, organic (HPC/CNC) and organic-inorganic bio-nanocomposites (HPC/CNCs/CeO_2) were investigated for the protection of wood surfaces housed in uncontrolled, outdoor environments. The application of thin bio-nanocomposite films onto the wood surface was achieved using the SBSp method. The SEM images highlight the positive results of this method, especially in the creation of uniform films. This is evident in the SEM analysis, where a thorough examination illustrates an even distribution of nanoparticles across the nanocomposite layer on the wood surface.

The findings, as revealed by FTIR analysis, demonstrate a reduction in photo-oxidation rates and an optimization of the stability of the HPC matrix through the incorporation of CNCs and CeO_2 nanofillers. ATR spectra comparisons of the treated wood surfaces before and after UV irradiation indicate that HPC/CNCs can partially shield the surface from UV light, and this protective effect is enhanced by introducing CeO_2 NPs into the bio-nanocomposite film.

The results clearly indicate that the addition of CNCs as a nanofiller to the HPC polymer provides partial protection against photochemical deterioration. This protective feature can be significantly improved by incorporating CeO_2 NPs into the matrix. The presence of CeO_2 in the films results in a narrower band gap, further enhancing their UV resistance. Additionally, analysis of UV-Vis spectra demonstrates that the bio-nanocomposite films with CeO_2 tend to absorb UV-A and UV-B regions more effectively than the pure organic matrices, contributing to their UV protection capabilities. Furthermore, the introduction of these new bio-nanocomposites results in reduced wettability of the coated wood, which may also contribute to a reduction in humidity induced wood degradation processes.

In conclusion, the organic-inorganic bio-nanocomposites studied here showed significant promise, compared to purely organic matrices, as compatible and effective treatments for the safeguarding of wood surfaces, particularly when exposed to outdoor conditions.

5. REFERENCES

1. Wimmers, G. Wood: a construction material for tall buildings. *Nature Reviews Materials* **2017,** *2*, 1-2.
2. Walsh-Korb, Z.; Avérous, L. Recent developments in the conservation of materials properties of historical wood. *Progress in Materials Science* **2019,** *102*, 167-221.
3. Walsh, Z.; Janeček, E.-R.; Hodgkinson, J. T.; Sedlmair, J.; Koutsioubas, A.; Spring, D. R.; Welch, M.; Hirschmugl, C. J.; Toprakcioglu, C.; Nitschke, J. R. Multifunctional supramolecular polymer networks as next-generation consolidants for archaeological wood conservation. *Proceedings of the National Academy of Sciences* **2014,** *111*, 17743-17748.
4. Florian, M.-L. E. Scope and history of archaeological wood. ACS Publications: **1990**.
5. Hon, D. N. S.; Chang, S. T. Surface degradation of wood by ultraviolet light. *Journal of Polymer Science: Polymer Chemistry Edition* **1984,** *22*, 2227-2241.
6. Feist, W. C. Outdoor wood weathering and protection. *Archaeological wood, properties, chemistry, and preservation. Advanced in Chemistry Series* **1990,** *225*, 263-298.
7. Cogulet, A.; Blanchet, P.; Landry, V. Wood degradation under UV irradiation: A lignin characterization. *Journal of Photochemistry and Photobiology B: Biology* **2016,** *158*, 184-191.
8. Petric, M. Surface modification of wood: a critical review. *Rev. Adhes. Adhes* **2013,** *1*, 216-47.
9. Hill, C. A. *Wood modification: chemical, thermal and other processes*. John Wiley & Sons: **2007**.

10. Yildiz, S.; Gümüşkaya, E. The effects of thermal modification on crystalline structure of cellulose in soft and hardwood. *Building and Environment* **2007,** *42*, 62-67.
11. Harandi, D.; Ahmadi, H.; Achachluei, M. M. Comparison of TiO2 and ZnO nanoparticles for the improvement of consolidated wood with polyvinyl butyral against white rot. *International Biodeterioration & Biodegradation* **2016,** *108*, 142-148.
12. Crisci, G. M.; La Russa, M. F.; Malagodi, M.; Ruffolo, S. A. Consolidating properties of Regalrez 1126 and Paraloid B72 applied to wood. *Journal of Cultural Heritage* **2010,** *11*, 304-308.
13. Christensen, M.; Kutzke, H.; Hansen, F. K. New materials used for the consolidation of archaeological wood–past attempts, present struggles, and future requirements. *Journal of Cultural Heritage* **2012,** *13*, S183-S190.
14. Salla, J.; Pandey, K. K.; Srinivas, K. Improvement of UV resistance of wood surfaces by using ZnO nanoparticles. *Polymer degradation and stability* **2012,** *97*, 592-596.
15. Frigione, M.; Lettieri, M. Novel attribute of organic–inorganic hybrid coatings for protection and preservation of materials (stone and wood) belonging to cultural heritage. *Coatings* **2018,** *8*, 319.
16. Nguyen, T.-P.; Lee, C.; Hassen, S.; Le, H. Hybrid nanocomposites for optical applications. *Solid State Sciences* **2009,** *11*, 1810-1814.
17. Ha, C. S. Polymer Based Hybrid Nanocomposites; A progress toward enhancing interfacial interaction and tailoring advanced applications. *The Chemical Record* **2018,** *18*, 759-775.
18. Baglioni, P.; Giorgi, R. Soft and hard nanomaterials for restoration and conservation of cultural heritage. *Soft matter* **2006,** *2*, 293-303.
19. Kanth, A. P.; Soni, A. K. Application of nanocomposites for conservation of materials of cultural heritage. *Journal of Cultural Heritage* **2023,** *59*, 120-130.
20. Clausen, C. A.; Green, F.; Nami Kartal, S. Weatherability and leach resistance of wood impregnated with nano-zinc oxide. *Nanoscale research letters* **2010,** *5*, 1464-1467.
21. Tuduce-Traistaru, A.-A.; Campean, M.; Timar, M. C. Compatibility indicators in developing consolidation materials with nanoparticle insertions for old wooden objects. *Int. J. Conserv. Sci* **2010,** *1*, 219-226.
22. Dong, Y.; Yan, Y.; Ma, H.; Zhang, S.; Li, J.; Xia, C.; Shi, S. Q.; Cai, L. In-situ chemosynthesis of ZnO nanoparticles to endow wood with antibacterial and UV-resistance properties. *Journal of Materials Science & Technology* **2017,** *33*, 266-270.
23. Feller, R. L.; Wilt, M. H. In *Evaluation of cellulose ethers for conservation*, **1990**.
24. Walsh, Z.; Janeček, E.-R.; Jones, M.; Scherman, O. A. Natural polymers as alternative consolidants for the preservation of waterlogged archaeological wood. *Studies in Conservation* **2017,** *62*, 173-183.
25. Ardelean, E.; Bobu, E.; Niculescu, G.; Groza, C. Effects of different consolidation additives on ageing behaviour of archived document paper. *Cellulose chemistry and technology* **2011,** *45*, 97.
26. Teper, J. H.; Straw, M. A survey of current leather conservation practices. *The Book and Paper Group Annual* **2011,** *30*, 1-151.
27. Younis, O. M.; El Hadidi, N. M.; Darwish, S. S.; Mohamed, M. F. Preliminary study on the strength enhancement of Klucel E with cellulose nanofibrils (CNFs) for the conservation of wooden artifacts. *Journal of Cultural Heritage* **2023,** *60*, 41-49.
28. Fulcher, K. An investigation of the use of cellulose-based materials to gap-fill wooden objects. *Studies in Conservation* **2017,** *62*, 210-222.
29. Caruso, M. R.; D'Agostino, G.; Milioto, S.; Cavallaro, G.; Lazzara, G. A review on biopolymer-based treatments for consolidation and surface protection of cultural heritage materials. *Journal of Materials Science* **2023,** 1-22.
30. Younis, O.; El Hadidi, N.; Darwish, S.; Mohamed, M. ENHANCING THE MECHANICAL STRENGTH OF KLUCEL E/CNC COMPOSITES FOR THE CONSERVATION OF WOODEN ARTIFACTS. *Egyptian Journal of Archaeological & Restoration Studies* **2023,** *13*.
31. Fico, D.; Rizzo, D.; Montagna, F.; Esposito Corcione, C. Fused Filament Fabrication and Computer Numerical Control Milling in Cultural Heritage Conservation. *Materials* **2023,** *16*, 3038.

32. Harandi, D.; Moradienayat, M. Multifunctional PVB nanocomposite wood coating by cellulose nanocrystal/ZnO nanofiller: Hydrophobic, water uptake, and UV-resistance properties. *Progress in Organic Coatings* **2023,** *179*, 107546.
33. Huang, R.; Du, X.; Wang, H.; Cheng, X.; Du, Z. Highly stretchable polyurethane coating based on functionalized cerium oxide nanoparticles for anti-corrosive/UV protection. *Journal of Applied Polymer Science* **2022,** *139*, 51927.
34. Bansal, R.; Nair, S.; Pandey, K. K. UV resistant wood coating based on zinc oxide and cerium oxide dispersed linseed oil nano-emulsion. *Materials Today Communications* **2022,** *30*, 103177.
35. Nair, S.; Nagarajappa, G. B.; Pandey, K. K. UV stabilization of wood by nano metal oxides dispersed in propylene glycol. *Journal of Photochemistry and Photobiology B: Biology* **2018,** *183*, 1-10.
36. Blanchard, V.; Blanchet, P. Color stability for wood products during use: Effects of inorganic nanoparticles. *BioResources* **2011,** *6*, 1219-1229.
37. Moradienayat, M.; Olmos, D.; González-Benito, J. Airbrushed Polysulfone (PSF)/Hydroxyapatite (HA) Nanocomposites: Effect of the Presence of Nanoparticles on Mechanical Behavior. *Polymers* **2022,** *14*, 753.
38. Ayadi, N.; Lejeune, F.; Charrier, F.; Charrier, B.; Merlin, A. Color stability of heat-treated wood during artificial weathering. *Holz als Roh-und Werkstoff* **2003,** *61*, 221-226.
39. Makuła, P.; Pacia, M.; Macyk, W. How to correctly determine the band gap energy of modified semiconductor photocatalysts based on UV–Vis spectra. ACS Publications: **2018**.
40. Mohammadian-Kohol, M.; Asgari, M.; Shakur, H. A detailed investigation of the gamma-ray radiation effects on the optical properties of polyvinyl butyral film. *Optik* **2016,** *127*, 7459-7468.
41. Mostafa, A. M. Preparation and study of nonlinear response of embedding ZnO nanoparticles in PVA thin film by pulsed laser ablation. *Journal of Molecular Structure* **2021,** *1223*, 129007.
42. Pandey, K. K. Study of the effect of photo-irradiation on the surface chemistry of wood. *Polymer degradation and Stability* **2005,** *90*, 9-20.
43. Pandey, K. A study of chemical structure of soft and hardwood and wood polymers by FTIR spectroscopy. *Journal of applied polymer science* **1999,** *71*, 1969-1975.
44. Wachter, I.; Štefko, T.; Rantuch, P.; Martinka, J.; Pokorny, J.; Blinová, L.; Ház, A.; Reinprecht, L. Comprehensive assessment of transparent wood degradation. *Polymer Testing* **2023,** *128*, 108206.
45. Zhang, J.; Zhang, D.; Zhang, X. UV-0/HPC laminated coatings for protection of cellulosed-based cultural heritage against UV rays. *Polymer Degradation and Stability* **2020,** *177*, 109169.
46. Nguyen, Q. B.; Pham, N. C.; Nguyen, T. H. C.; Doan, T. D.; Duong, T. L.; Pham, N. N.; Nguyen, V. N. M.; Dao, N. N. Porous nonhierarchical CeO2-SiO2 nanocomposites for improving the ultraviolet resistance capacity of polyurethane coatings. *Materials Research Express* **2021,** *8*, 056405.
47. Abd-Elrahman, M. I.; Ahmed, M. O.; Abdel-Aleem, J. A. Optical properties of cellulose derivatives blend film carrying a chalcogenide material. *Materials science in semiconductor processing* **2013,** *16*, 1052-1056.
48. Aziz, S. B.; Dannoun, E. M.; Tahir, D. A.; Hussen, S. A.; Abdulwahid, R. T.; Nofal, M. M.; M. Abdullah, R.; M. Hussein, A.; Brevik, I. Synthesis of PVA/CeO2 based nanocomposites with tuned refractive index and reduced absorption edge: Structural and optical studies. *Materials* **2021,** *14*, 1570.
49. Makuła, P.; Pacia, M.; Macyk, W. How to correctly determine the band gap energy of modified semiconductor photocatalysts based on UV–Vis spectra. ACS Publications: **2018**; Vol. 9, pp 6814-6817.
50. Nagarajappa, G. B.; Pandey, K. K. UV resistance and dimensional stability of wood modified with isopropenyl acetate. *Journal of Photochemistry and Photobiology B: Biology* **2016,** *155*, 20-27.
51. Wang, X.; Chai, Y.; Liu, J. Formation of highly hydrophobic wood surfaces using silica nanoparticles modified with long-chain alkylsilane. *Holzforschung* **2013,** *67*, 667-672.